Jurnal Riset Kimia

ISSN (print) : 1978-628X
ISSN (online) : 2476-8960

Black Water Purification by Activated Carbon from Ilalang Weeds (I*mperata cylindrica*) Adsorbent in Peatland Rural Area

Ngatijo[a*], Heriyanti[a], Winda Arinda Putri[a], Aslan Irunsah[b], Bayu Ishartono[b], and Rahmat Basuki[c]
[a]Department of Chemistry, Faculty of Science and Technology, Universitas Jambi, Jambi, Indonesia
[b]Bureau of School Curriculum Analysis, Design, and Interpretation, Master of Chemistry Alumny Forum (FAMK), Universitas Gadjah Mada, Yogyakarta, Indonesia
[c]Department of Chemistry, Faculty of Military Mathematics and Natural Sciences, Universitas Pertahanan RI, Bogor, West Java, Indonesia

Corresponding Author:
Ngatijo
tijo52@yahoo.co.id

Received: August 2021
Accepted: November 2021
Published: March 2022

Abstract

The black water containing humic acid, HA in peat land rural area is a serious issue. This study aims to synthesis of activated carbon, AC from Ilalang Weeds, IW (*Imperata cylindrica*) as low-cost adsorbent for HA. The success AC synthesis by H_3PO_4 activator from IW was evidently characterized by Fourier Transform Infra-Red, FTIR and Scanning Electron Microscopy, SEM. The effects of pH solution, initial HA concentration, and contact time were systematically studied to investigate the performance of Activated Carbon from Ilalang Weeds, ACIW. The results showed the increasing of Langmuir monolayer capacity of HA adsorption on carbon from IW before (49.75 mg g^{-1}) and after (56.82 mg g^{-1}) activation process at the pH optimum 6.0. The equilibrium adsorption data fitted with the isotherm model was shifted from multilayer Freundlich model (CIW) into monolayer Langmuir model as the consequences of increasing pore diameter size and active sites intensity. Calculation of adsorption energy by Dubinin-Radushkevich (E_{DR}) model, 0.50 and 2.24 kJ mol^{-1} for CIW and ACIW, respectively, showed the increasing of physical affinity of HA with the active sites of adsorbent. Adsorption kinetics showed that the adsorption behavior followed the Ho pseudo-second-order kinetic model. The experimental results of this work demonstrate that the ACIW can be used as a promising low-cost adsorbent for HA removal for clean water production in peat land rural area.

Keywords: *activated carbon; adsorption; H_3PO_4 activator; humic acid (HA); low-cost adsorbent*

Introduction

The need for clean water for people in peat lands rural area in Jambi Province is a serious problem to date[1]. The condition of water is dark brown, acidic, and high content humic acid (HA)[2]. HA has abundant functional groups such as phenolic, ketone, carboxylic, amine, and peptide group (Figure 1)[3]. HA contained water gives a bad smell and taste of water that have potential to cause problems for human health. HA also tends to interact with pollutant to form carcinogenic compounds such as trihalomethane and haloacetic acid[4]. Therefore, serious efforts are required to overcome this issue.

DOI: https://doi.org/10.25077/jrk.v13i1.449

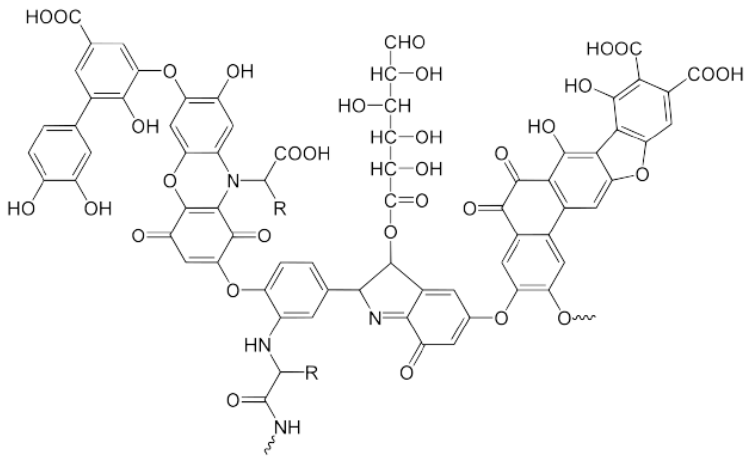

Figure 1. Structure of humic acids (HA)[3].

Several methods have been developed to overcome the issue, including membrane filtration[5], reverse osmosis[6], photodegradation[7], and adsorption[8]. The adsorption method still become promising method due to its simple operation, safe, and cheap[9]. The use of adsorbents in the adsorption of HA in peat water has been widely reported, including the use of pyrophyllite[4], powdered eggshell[10], and coconut copra residue[11]. To date the use of adsorbents that are easy to synthesize, cheap, and derived from abundant materials without compromising performance are still highly attracts researchers. One of the materials that meet these criteria is activated carbon, AC. The production of AC from green, low-price, and renewable source is growing interest of researcher: cassava leaves[12], rubber fruit shell[13], sengon wood (*Paraserianthes falcataria*) shaws powder[14], sugarcane dregs[15], durian peel[16], coconut shell[17], and enceng gondok plant[18]. One of the plant that are abundant, high in availability, and cheap is Ilalang Weeds (*Imperata cylindrical*).

Ilalang Weeds (*Imperata cylindrical*), IW are reported to contain relatively high levels of cellulose, hemicellulose, and lignin[19]. Therefore, IW considered having promising prospects due to its abundance in nature and its presence as a weed. However, the utilization of IW as a source of AC had limitedly found in literature. This study aims to develop AC from IW, ACIW as HA adsorbent in the peat water purification. The development of ACIW includes a carbonization process and activation process by H_3PO_4 that reported can remove the impurities[20][21][22]. The use of H_3PO_4 activator in the activation process is expected to increase the number of active sites that play important role in the HA adsorption process. The performance of the synthesized ACIW to adsorb HA has been studied by the isotherm and kinetics parameters at the optimum pH.

Experimental

Materials

Dry and clean Ilalang Weeds (IW) from the Mendalo, Jambi has been prepared. All chemicals is *pro analyst* produced from Merck® (H_3PO_4 85%, HNO_3 65%, and NaOH pellets) and HA sample produced from Sigma-Aldrich.

Instruments

Quantification of HA was performed by UV-Vis Spectrophotometer Perkin Elmer Lambda 35 and the characterization of functional group was conducted by Fourier Transform-Infrared Spectrometer (FTIR) Perkin Elmer Frontier. The diameter pore size and morphological of synthesized ACIW was characterized by

Scanning Electron Microscope (SEM) Hitachi Flexsem 1000.

Preparation of activated carbon from Ilalang Weed (ACIW)

The ACIW has been produced through carbonization by 300 °C furnace for 2 h and activation steps by H_3PO_4 10% according to a modified previous study[23].

HA adsorption study

Effect of pH

Effect of pH has been studied by variation of pH medium at 3, 4, 5, 6, 7, and 8. The pH was adjusted by addition of 0.1 M HNO_3 and 0.1 M NaOH. The adsorbed HA was measured by UV-Vis spectrophotometer (UV-1800 Shimadzu) at maximum λ, 205 nm and calculated using Eq. (1):

$$q_e = \frac{(C_0 - C_e)v}{w} \quad (1)$$

Isotherm study

The isotherm study was conducted by the adsorption of 50 mL of varied HA initial concentration (30, 50, 70, 90, 120, and 150 mg L^{-1} at optimum pH) onto 100 mg ACIW (or CIW) for 180 min. The adsorbed HA was calculated by Eq. (1). The data was applied to isotherm model: Langmuir (Eq.2)[24], Freundlich (Eq.3)[25], and Dubinin-Radushkevich, D-R[26] (Eq.4) in order to determine the isotherm corresponding parameters.

$$\frac{C_e}{q_e} = \frac{1}{bK_L} + \frac{1}{b}C_e \quad (2)$$

$$\ln q_e = \ln B + \frac{1}{n}\ln C_e \quad (3)$$

$$\ln q_e = \ln q_{DR} - B_{DR}\varepsilon^2 \quad (4)$$

Kinetics study

The kinetics study was conducted by contacting 100 mg of ACIW with 50 mL of 95 mg L^{-1} HA solution for 10 min. A similar step was conducted with variations in contact time: 20, 30, 45, 60, and 90 min. The kinetics data was applied into kinetics models: Lagergren[27], pseudo-first order (Eq.5), Ho[28], pseudo-second order (Eq.6), and proposed Rusdiarso-Basuki-Santosa, RBS second order model[25],[29]–[32] (Eq.7).

$$\ln(q_e - q_t) = \ln q_e - k_{Lag}t \quad (5)$$

$$\frac{t}{q_t} = \frac{1}{k_{Ho}q_e^2} + \frac{1}{q_e}t \quad (6)$$

$$\ln\left(\frac{C_0C_b - x_e x}{x_e - x}\right) = k_a\left(\frac{C_0C_b - x_e^2}{x_e}\right)t - \ln\left(\frac{x_e}{C_0C_b}\right) \quad (7)$$

Result and Discussion

Preparation of ACIW

The carbonization process was conducted by incomplete combustion to decompose cellulose and lignin with a limited supply of oxygen to produce black carbon according to the following reactions (Eq. 8 and 9)[33]:

$$C_nH_{2n+2(s)} + O_{2(g)} \rightarrow nCO_{(g)} + (n+1)H_2O_{(g)} \quad (8)$$

$$C_nH_{2n+2(s)} + O_{2(g)} \rightarrow nC_{(s)} + (n+1)H_2O_{(g)} \quad (9)$$

The activation reaction mechanism using H_3PO_4 solution on carbon is presented in the schematic in Figure 2[34]. The oxygen of the PO_4^{3-} anions activator binds to the carbon by releasing the hydroxyl group on the carbon. This causes the impurity that covers the surface of the ACIW pores to decrease. Thus, this can increase its adsorption capacity[34].

 DOI: https://doi.org/10.25077/jrk.v13i1.449

Characterization of ACIW

The absorption spectra of carbon from IW before the activation process (CIW) were presented in Figure 3(a). It was shown that there was no significant peak indicated the CIW has few functional groups.

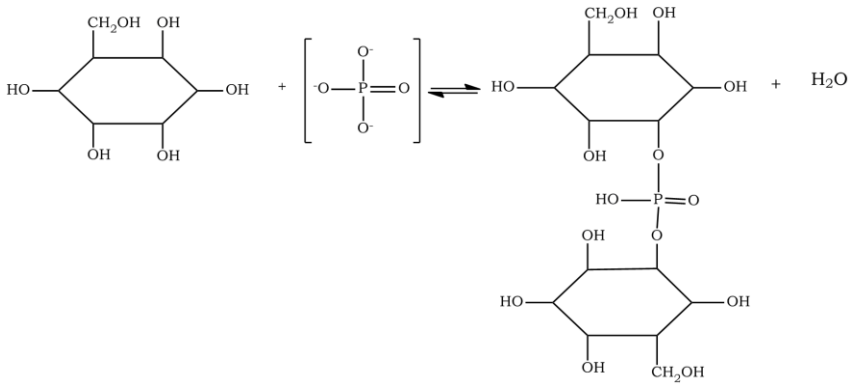

Figure 2. Schematic representation of the IW carbon-H_3PO_4[34].

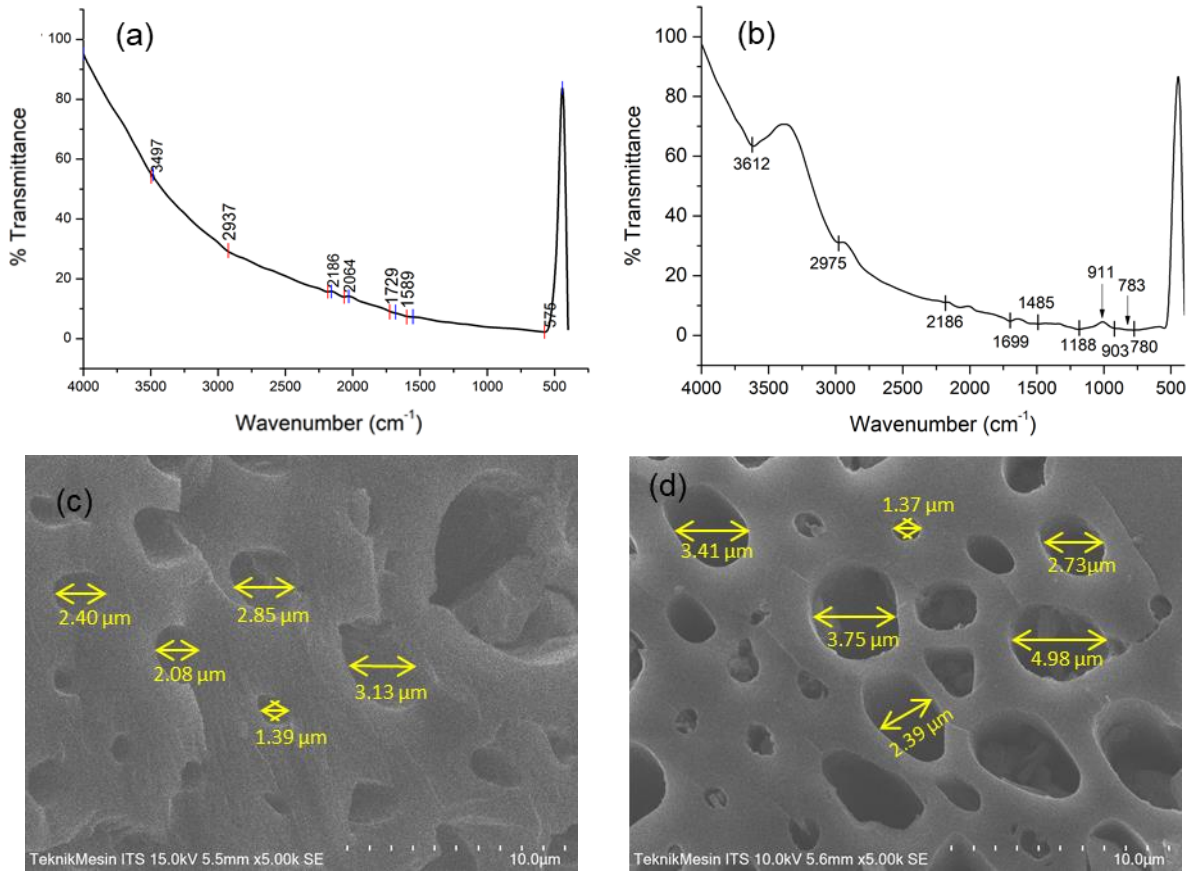

Figure 3. The FTIR spectra of carbon from IW before (CIW) (a) and after activation (ACIW) (b) and SEM image of image CIW (c) and ACIW (d).

However, the weak absorption were detected at 3497, 2937, 2186, 1729, and 1589 cm-1 that indicated the vibration of O-H stretching, C-H stretching, C≡C stretching, C=O stretching, and C=C stretching, respectively[35]. After the activation process, it was observed that there was increasing the intensity of the peak of ACIW (Figure 3(b)). The absorption band of ACIW at 3612 cm^{-1} was attributed to the O-H stretching vibrations of carboxylic groups, phenols, and alcohols[36]. The band at 2186 and 1485 cm^{-1} can be assigned to C≡C, and C=C stretching vibration, respectively. The band at 1699 and 1188 cm^{-1} was ascribed to C=O stretching vibration and phosphorus/oxygen compounds, respectively. This is due to the activation with H_3PO_4 which overlaps with the C-O stretching vibrations of the acid, alcohol, phenol, ether, and ester groups[21]. New bands at 911 and 783 cm^{-1} appeared after shifting from 903 and 780 cm^{-1} (Figure 3(b)) were assigned to aromatic C-H vibration of ACIW.

A surface morphology analysis by SEM exhibited the increasing of diameter pore size between CIW (1.39-3.13 μm) and ACIW (1.37-4.98 μm) that showed in Figure 3(c) and 3(d), respectively. This indicates the success activation process of CIW by the H_3PO_4 solution. The synthesized ACIW has the potential of higher adsorption capacity as an HA adsorbent due to larger size pores. Higher pore diameter size makes ACIW have a larger surface area so that the number of active sites also increases as shown in Figure 3(b). Several report showed the increasing of pore size and surface area was in line with the increasing of adsorption capacity of the synthesized AC[14],[16],[37],[38].

Determining of optimum pH

pH is essential features in adsorption process due to the changes in the charge distribution of the ACIW and HA as a result of protonation and de-protonation reactions of functional groups[39][25]. The result of the optimization of pH effect was shown in Figure 5. From the Figure 5, in all pH range the HA adsorbed was above 80 mg L^{-1} and the optimum pH was observed at pH 6.0. From this pattern, it can be deducted that pH had no significant effect to the HA adsorption onto ACIW. This often occurs in adsorption processes that have physical interactions mechanisms[40].

Isotherm study

The adsorption of HA onto ACIW and CIW was increased with increasing C_0 from 30 to 120 mg/L and reached the equilibrium at 180 min with no further adsorbed HA. The plot of isotherm data to the isotherm model as presented in Figure 6 and the calculated corresponding isotherm parameter was listed in Table 1. By correlating the linearity value (R^2) of the isotherm models in Table 1, the Langmuir and Freundlich model show the best representative model for the HA adsorption onto ACIW and CIW, respectively.

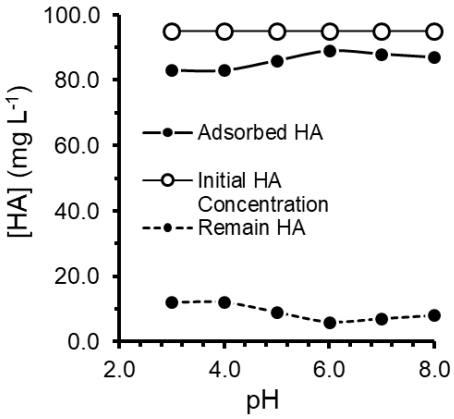

Figure 5. The effect of HA solution pH on the HA adsorption onto ACIW

 DOI: https://doi.org/10.25077/jrk.v13i1.449

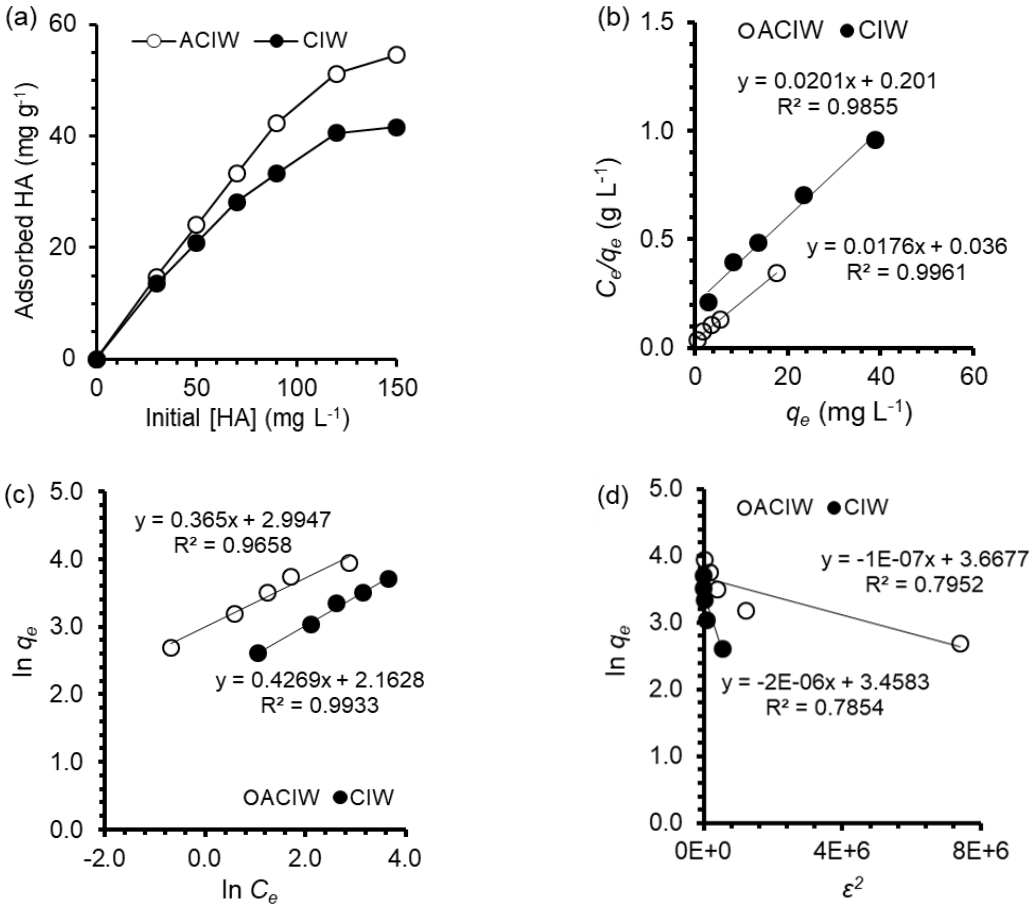

Figure 6. The effect of initial HA concentration on adsorbed HA onto ACIW and CIW (a); The plot of isotherm data of HA adsorption onto ACIW and CIW on the Langmuir (b), Freundlich (c), and D-R (d) isotherm model.

Table 1. Comparison of isotherm parameter of HA adsorption onto CIW and ACIW

Adsorbents	Langmuir			Freundlich			D-R		
	b (mg g^{-1})	*K* (L mg^{-1})	R^2	*n*	*B* (mg g^{-1})	R^2	q_{D-R} (mg g^{-1})	B_{D-R}	R^2
ACIW	56.82	0.49	0.9961	2.74	19.98	0.9658	39.13	1.0×10^{-7}	0.7952
CIW	49.75	0.09	0.9855	2.34	8.70	0.9933	31.76	2.0×10^{-6}	0.7854

The fitted isotherm to the data was changed from Freundlich (HA onto CIW) into Langmuir model (HA onto ACIW). This indicates that ACIW has the uniform active sites after the activation step. Before the activation process, CIW has heterogenic sites to bind with HA. The result strengthens the fact that there was increasing diameter pore size and functional group intensity showed in Figure 3.

The important features of the Langmuir model can be expressed in terms of dimensionless

constant called separation factor of equilibrium parameter, R_L described by Weber and Cakkravorti[41]:

$$R_L = \frac{1}{1 + K_L C_0} \quad (10)$$

which the R_L values indicated to irreversible (R_L=0), favorable (0<R_L<1), and unfavorable (R_L>1). The calculated R_L in this work was ranged from 0.06-0.02 for ACIW and 0.27-0.09 for CIW that indicate the adsorptions were favorable.

The increasing in monolayer adsorption capacity of HA adsorption onto CIW (49.75 mg g^{-1}) and ACIW (56.82 mg g^{-1}) was also evidently proved that activation process was increasing the active sites of carbon from IW. The value of CIW and ACIW adsorption capacity was quite higher than adsorption capacity of HA adsorbent from natural zeolites (0.2787 mg g^{-1})[42], natural zeolites/TiO_2 (1.199 mg g^{-1})[42], untreated AC (19 mg g^{-1})[43], H_3PO_4 treated AC (26 mg g^{-1})[43], H_2SO_4 treated AC (20 mg g^{-1})[43], magnetic Zn/Al CLDH (165.84 mg g^{-1})[44], HNO_3 treated granular AC (58.83 mg g^{-1})[45], and powder AC (76.92 mg g^{-1})[45].

The D-R isotherm is able to estimate the adsorption mechanism by calculated the adsorption energy (E_{D-R}). E_{D-R} can be calculated by $(2B_{D-R})^{-1/2}$. The calculated E_{D-R} in this work was 2.24 kJ mol^{-1} (ACIW) and 0.5 kJ mol^{-1} (CIW) that indicate the adsorption occurred through physical interaction between HA onto ACIW and CIW, respectively. The E_{D-R} showed that the HA has stronger interaction with ACIW than CIW due to the higher content of functional group of ACIW compared with CIW. This based on the categorize that if the value of E_{D-R} is <8 kJ mol^{-1} the adsorption type can be explained by physical adsorption, between 8 and 16 kJ mol^{-1} is ion exchange interaction, and >16 kJ mol^{-1} is chemical adsorption[46],[47].

This mechanism can be observed by FT-IR and SEM analysis of ACIW-HA after adsorption process (Figure 7). The difference in functional groups between the FTIR spectrum of ACIW before and after adsorption showed from decreasing in the absorption followed by a shift at 3728 cm^{-1} indicates that O-H groups have interacted with HA after adsorption (Figure 7a). The shift of the aliphatic C-H stretching vibration from 2975 to 2984 cm^{-1} indicates that ACIW has interacted with HA. It is predicted that the interaction of ACIW with HA occurs in the pores of ACIW (Figure 7b).

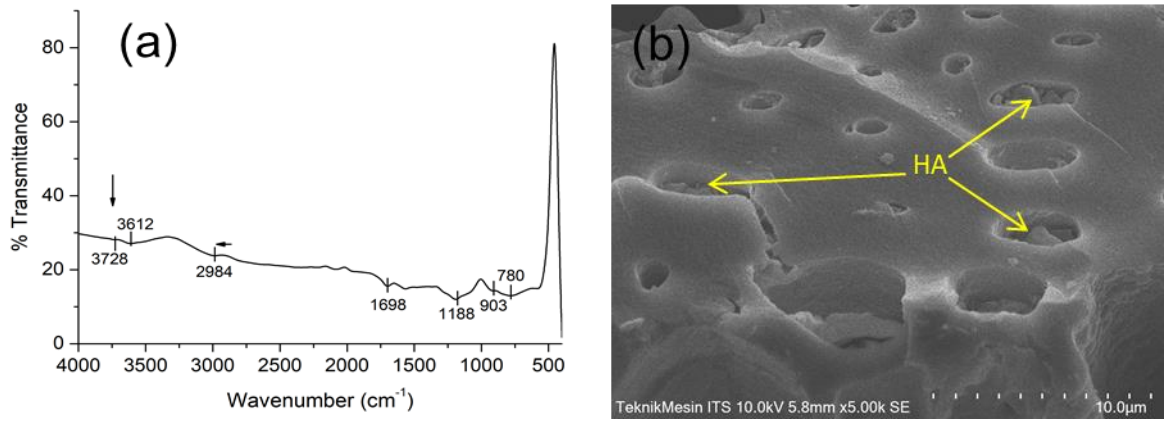

Figure 7. The FT-IR spectra (a) and SEM image with 5000× magnification (b) of ACIW-HA.

 DOI: https://doi.org/10.25077/jrk.v13i1.449

Kinetics study

The adsorption rates of HA onto ACIW was rapidly occurred at the first 15 min, and then slow down until the equilibrium is reached at 120 min (Figure 8a). The rapid HA adsorption onto ACIW active sites indicates HA compatibility with ACIW's active sites after activation process. The adsorbed HA onto ACIW was presented in Figure 7. The slow step of first 15 min adsorption possibly caused by the slightly difference in concentration gradient. The increasing HA adsorption on ACIW was due to the occupying a free site or pores of ACIW that characterized in Figure 3. Thereafter, as times continue, the free sites got saturated and reached the equilibrium. In this study, the adsorbed HA on ACIW was found to be 26.25 mg g^{-1} (equal to 8.75×10^{-8} mol g^{-1} based on the referred molecular weight of HA by MacFarlane and Bruch[48]). The plot of kinetics data to the kinetics models was presented in Figure 8b-8d and the corresponding parameters were listed in Table 2.

The linearity value (R^2) comparison between three kinetics model in Figure 8 showed the best model to represent HA adsorption onto ACIW is Ho model (R^2=1.00). Further, the calculation of q_e ($q_{e,\ calc}$) of Ho (26.88 mg g^{-1}) (Table 2) was also the closest value to the experimental q_e ($q_{e,\ exp}$=26.25 mg g^{-1}) in this work. This indicates that the adsorption process follows the pseudo-second-order mechanism. Further observation, the proposed RBS kinetics models possible to generate the desorption rate constant (k_d) and through $K_{RBS}=k_a/k_d$ relationship, the Gibbs free energy (ΔG) can be calculated from $\Delta G=-RT \ln K_{RBS}$. The result of ΔG calculation found in this work was 36.30 (ΔG<40 kJ mol^{-1}) that indicate the physical interaction[49].

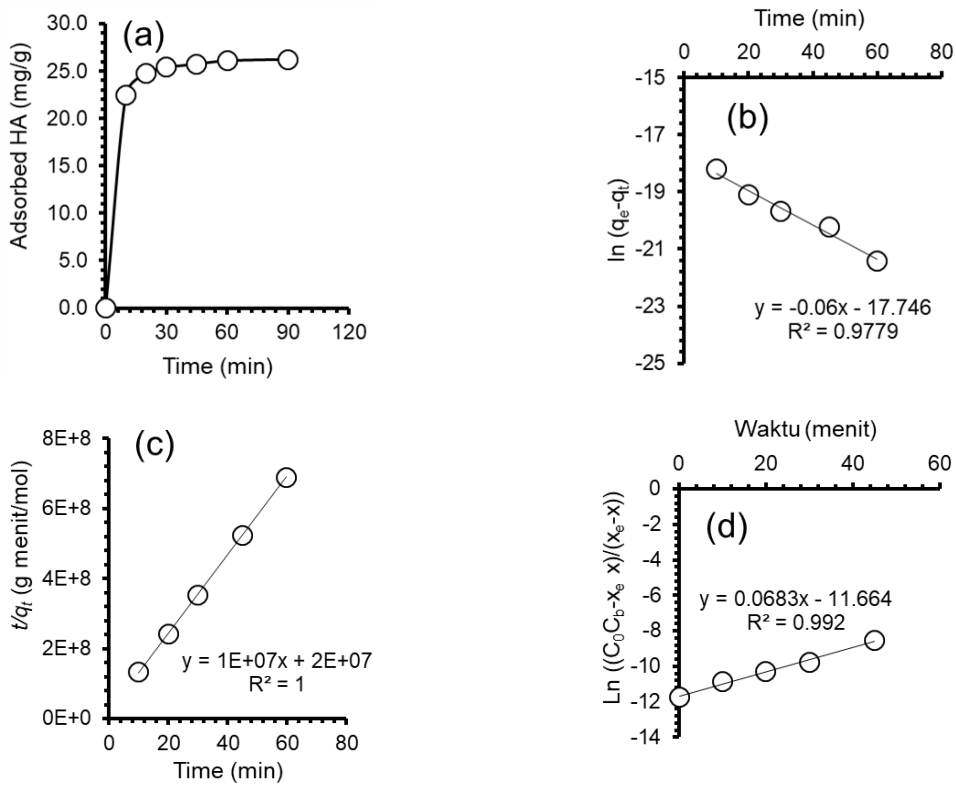

Figure 8. Profile of adsorbed HA onto ACIW as a function of time (a); Plot of kinetics data to the Lagergren (b), Ho (c), and RBS (d) kinetics model.

Table 2. Corresponding parameters value of HA adsorption onto ACIW

Kinetics Models	Kinetics Parameters					
	k_{Lag} (min^{-1})	k_{Ho} (g mol^{-1} min^{-1})	k_a (L mol^{-1} min^{-1})	k_d (min^{-1})	$q_{e,\,calc}$ (mg g^{-1})	R^2
Lagergren	0.06	-	-	-	5.89	0.98
Ho	-	6.05×10^{6}	-	-	26.88	1.00
RBS	-	-	6.15×10^{4}	2.66×10^{-2}	3.92	0.99

Conclusion

Synthesis of activated carbon from Ilalang weeds (*Imperata cylindrica*) using H_3PO_4 activator as a low cost HA adsorbent has been successfully performed. The success synthesis was evidently by increasing the intensity of the ACIW active sites and increasing in pore diameter size of ACIW. The optimum condition of HA adsorption was occurred at pH 6.0. Under the optimum condition, the monolayer adsorption capacity of HA uptake was increase from 49.75 (CIW) to 56.82 (ACIW) mg g^{-1} with the D-R adsorption energy of 0.50 and 2.24 kJ mol^{-1}, respectively, that indicate physical adsorption process. Kinetics study of HA uptake was follows the Ho pseudo-second-order kinetics mechanism. The performances of ACIW demonstrate that the ACIW is a promising low-cost adsorbent for HA removal for clean water production in peat land rural area.

Acknowledgment

The authors thanks to Universitas Jambi through PTUPT Program (No Contract: 2653/UN21.18/PG/SPK/2020) for financing this work.

Abbreviation list	
B	multilayer adsorption capacity (mg/g)
b	monolayer adsorption capacity (mg/g)
B_{DR}	D-R free energy (mol^2/J^2)
C_b	concentration of monolayer capacity [C_b=bw/v] (mol/L)
C_e	HA final concentration (mg/L)
ε	initial HA concentration (mg/L)
k_a	Polanyi potential [ε = RT ln (1+1/C_e)] (J^2/mol^2)
k_d	RBS rate constants (L/mol min)
k_{Ho}	RBS desorption rate constant (min^{-1})
k_{Lag}	Ho rate constant (g/mol min)
K_L	Lagergren rate constant (min^{-1})
q_{DR}	Langmuir constant (L/mol)
q_e	D-R isotherm capacity (mg/g)
v	adsorbed HA (mg/g)
w	volume (L)
x	weight (g)
x_e	adsorbed HA at time t (mol/L)
	adsorbed HA at time equilibrium (mol/L)

References

1. Chaidir, Z., Hasanah, Q. & Zein, R., Penyerapan ion logam Cr (III) dan Cr (VI) dalam larutan menggunakan kulit buah jengkol (Pithecellobium jiringa (Jack) Prain.). *J. Ris. Kim.*, **8(2)**: 189 (2015).
2. Hasnirwan., Aziz, H. & Whulanda, R., Sistem biofiltrasi air rawa gambut dan pengaruh filtrasi terhadap pH, BOD, COD, TSS dan asam humat air rawa gambut dengan adanya penambahan karbon. *J. Ris. Kim.*, **3(1)**: 54 (2015).
3. Joshi, R., Singh, J. & Vig, A. P., Vermicompost as an effective organic fertilizer and biocontrol agent: effect on growth, yield and quality of plants. *Rev. Environ. Sci. Biotechnol.*, **14(1)**: 137–159 (2015).

 DOI: https://doi.org/10.25077/jrk.v13i1.449

4. Zulfikar, M. A. & Setiyanto, H., Adsorption of humic acid from peat water on pyrophyllite. *Int. J. Chem. Environ. Biol. Sci.*, **1(4)**: 714–717 (2013).
5. Luo, X., Liang, H., Qu, F., Ding, A., Cheng, X., Tang, C. Y. & Li, G., Free-standing hierarchical α-MnO2@CuO membrane for catalytic filtration degradation of organic pollutants. *Chemosphere*, **200**: 237–247 (2018).
6. Pérez-González, A., Urtiaga, A. M., Ibáñez, R. & Ortiz, I., State of the art and review on the treatment technologies of water reverse osmosis concentrates. *Water Res.*, **46(2)**: 267–283 (2012).
7. Iovino, P., Chianese, S., Canzano, S., Prisciandaro, M. & Musmarra, D., Photodegradation of diclofenac in wastewaters. *Desalin. Water Treat.*, **61(2)**: 293–297 (2017).
8. Rusdiarso, B. & Basuki, R., Stability improvement of humic acid as sorbent through magnetite and chitin modification. *J. Kim. Sains dan Apl.*, **23(5)**: 152–159 (2020).
9. Chianese, S., Fenti, A., Iovino, P., Musmarra, D. & Salvestrini, S., Sorption of organic pollutants by humic acids: A review. *Molecules*, **25(4)**: 918 (2020).
10. Zulfikar, M. A., Novita, E., Hertadi, R. & Djajanti, S. D., Removal of humic acid from peat water using untreated powdered eggshell as a low cost adsorbent. *Int. J. Environ. Sci. Technol.*, **10(6)**: 1357–1366 (2013).
11. Sim, S. F., Lee, T. Z. E., Mohd Irwan Lu, N. A. L. & Murtedza, M., Modified coconut copra residues as a low cost biosorbent for adsorption of humic substances from peat swamp runoff. *BioResources*, **9(1)**: 952–968 (2014).
12. Maulinda, L., Nasrul, Z. A. & Sari, D. N., Pemanfaatan kulit singkong sebagai bahan baku karbon aktif. *J. Teknol. Kim. Unimal*, **4(2)**: 11–19 (2017).
13. Efiyanti, L., Wati, S. A. & Maslahat, M., Pembuatan dan analisis karbon aktif dari cangkang buah karet dengan proses kimia dan fisika. *J. Ilmu Kehutan.*, **14(1)**: 94–108 (2020).
14. Erawati, E. & Fernando, A., Pengaruh jenis aktivator dan ukuran karbon aktif terhadap pembuatan adsorbent dari serbik gergaji kayu sengon (Paraserianthes falcataria). *J. Integr. Proses*, **7(2)**: 58–66 (2018).
15. Sari, M. F. P., Loekitowati, P. & Moehadi, R., Penggunaan karbon aktif dari ampas tebu sebagai adsorben zat warna procion merah dari industri songket. *J. Pengelolaan Sumberd. Alam dan Lingkung. (Journal Nat. Resour. Environ. Manag.*, **7(1)**: 37–40 (2017).
16. Husin, A. & Hasibuan, A., Studi pengaruh variasi konsentrasi asam posfat (H3PO4) dan waktu perendaman karbon terhadap karakteristik karbon aktif dari kulit durian. *J. Tek. Kim. USU*, **9(2)**: 80–86 (2020).
17. Hakim, L. & Sedyadi, E., Synthesis and characterization of Fe3O4 composites embeded on coconut shell activated carbon. *JKPK (Jurnal Kim. dan Pendidik. Kim.*, **5(3)**: 245–253 (2020).
18. Nuria, F. I., Anwar, M. & Purwaningsih, D. Y., Pembuatan karbon aktif dari enceng gondok. *J. TECNOSCIENZA*, **5(1)**: 37–48 (2020).
19. Pratama, B. S., Konversi ampas tebu menjadi biochar dan karbon aktif untuk penyisihan Cr (VI). *J. Rekayasa Bahan Alam dan Energi Berkelanjutan*, **2(1)**: 7–12 (2018).
20. Koleangan, H. S. J. & Wuntu, A. D., Kajian stabilitas termal dan karakter kovalen zat pengaktif pada arang aktif limbah gergajian kayu meranti (Shorea spp). *Chem. Prog.*, **1(1)**: 43–46 (2008).
21. Budinova, T., Ekinci, E., Yardim, F., Grimm, A., Björnbom, E., Minkova, V. & Goranova, M., Characterization and application of activated carbon produced by H3PO4 and water vapor activation. *Fuel Process. Technol.*, **87(10)**: 899–905 (2006).
22. Yang, Z., Gleisner, R., Mann, D. H., Xu, J., Jiang, J. & Zhu, J. Y., Lignin based activated carbon using H3PO4 activation. **12(12)**: 1–16 (2020).
23. Ngatijo, N., Permana, E., Yanti, L. P., Ishartono, B. & Basuki, R., Remazol

briliant blue uptake by green and low-price black carbon from ilalang weeds (Imperata cylindrica) activated by KOH solution. *KPK (Jurnal Kim. dan Pendidik. Kim.*, **6(2)**: 192–205 (2021).

24. Basuki, R., Yusnaidar, Y. & Rusdiarso, B., Different style of Langmuir isotherm model of non-competitive sorption Zn(II) and Cd(II) onto horse dung humic acid (HD-HA). *AIP Conf. Proc.*, **2026**: 020009 (2018).
25. Basuki, R., Rusdiarso, B., Santosa, S. J. & Siswanta, D., Magnetite-functionalized horse dung humic acid (HDHA) for the uptake of toxic lead (II) from artificial wastewater. *Adsorpt. Sci. Technol.*, **2021(5523513)**: 1–15 (2021).
26. Dubinin, M. M. & Radushkevich, L. V., The equation of the characteristic curve of the activated charcoal USSR. *Proc. Acad. Sci. Phys. Chem. Sect.*, **55**: 331–337 (1947).
27. Lagergren, S., About the theory of so-called adsorption of soluble substances. *Sven. Vetenskapsakad. Handingarl*, **24**: 1–39 (1898).
28. Ho, Y. S., McKay, G., Wase, D. A. J. & Forster, C. F., Study of the sorption of divalent metal ions on to peat. *Adsorpt. Sci. Technol.*, **18(7)**: 639–650 (2000).
29. Rusdiarso, B., Basuki, R. & Santosa, S. J., Evaluation of lagergren kinetics equation by using novel kinetics expression of sorption of Zn2+ onto horse dung humic acid (HD-HA). *Indones. J. Chem*, **16(3)**: 338–346 (2016).
30. Basuki, R., Ngatijo., Santosa, S. J. & Rusdiarso, B., Comparison the new kinetics equation of noncompetitive sorption Cd(II) and Zn(II) onto green sorbent horse dung humic acid (HD-HA). *Bull. Chem. React. Eng. Catal.*, **13(3)**: 475–488 (2018).
31. Ngatijo, N., Basuki, R., Rusdiarso, B. & Nuryono, N., Sorption-desorption profile of Au (III) onto silica modified quaternary amines (SMQA) in gold mining effluent. *J. Environ. Chem. Eng.*, **8(3)**: 103747 (2020).
32. Ngatijo, N., Gusmaini, N., Bemis, R. & Basuki, R., Adsorpsi methylene blue pada nanopartikel magnetit tersalut asam humat: kajian isoterm dan kinetika. *CHEESA Chem. Eng. Res. Artic.*, **4(1)**: 51–64 (2021).
33. Desi., Suharman, A. & Vinsiah, R., Pengaruh variasi suhu karbonisasi terhadap daya serap karbon aktif cangkang kulit buah karet (Hevea brasilliensis). in *Prosiding SEMIRATA 2015 bidang MIPA BKS-PTN Barat*, 294–303 (2015).
34. Esterlita, M. O. & Herlina, N., Pengaruh penambahan aktivator ZnCl2, KOH, dan H3PO4 dalam pembuatan karbon aktif dari pelepah aren (Arenga pinnata). *J. Tek. Kim. USU*, **4(1)**: 47–52 (2015).
35. Mirzapour, P., Kamyab Moghadas, B., Tamjidi, S. & Esmaeili, H., Activated carbon/bentonite/Fe3O4 nanocomposite for treatment of wastewater containing Reactive Red 198. *Sep. Sci. Technol.*, **56(16)**: 2693–2707 (2021).
36. Hidayati, A., Kurniawan, S., Restu, N. W. & Ismuyanto, B., Potensi ampas tebu sebagai alternatif bahan baku pembuatan karbon aktif. *Nat. B*, **3(4)**: 311–317 (2016).
37. Heidarinejad, Z., Dehghani, M. H., Heidari, M., Javedan, G., Ali, I. & Sillanpää, M., Methods for preparation and activation of activated carbon: a review. *Environ. Chem. Lett.*, **18(2)**: 393–415 (2020).
38. Hanum, F., Gultom, R. J. & Simanjuntak, M., Adsorpsi zat warna metilen biru dengan karbon aktif dari kulit durian menggunakan KOH dan NAOH sebagai aktivator. *J. Tek. Kim. USU*, **6(1)**: 49–55 (2017).
39. Zam Zam, Z., Limatahu, N. A. & Baturante, N. J., Nitrate adsorption capacity of activated gamalama volcanic ash. *JKPK (Jurnal Kim. dan Pendidik. Kim.*, **6(1)**: 23 (2021).
40. Illés, E. & Tombácz, E., The effect of humic acid adsorption on pH-dependent surface charging and aggregation of magnetite nanoparticles. *J. Colloid Interface Sci.*, **295(1)**:

115–123 (2006).

41. Weber, T. W. & Chakravorti, R. K., Pore and solid diffusion models for fixed-bed adsorbers. *AIChE J.*, **20(2)**: 228–238 (1974).
42. Septiani, U., Tasari, F. J. & Zilfa, Z., Adsorpsi asam humat pada zeolit alam yang dimodifikasi dengan TiO2. *J. Ris. Kim.*, **11(1)**: 43–51 (2020).
43. Islam, M. A., Morton, D. W., Johnson, B. B. & Angove, M. J., Adsorption of humic and fulvic acids onto a range of adsorbents in aqueous systems, and their effect on the adsorption of other species: A review. *Separation and Purification Technology*, **247**: 116949 (2020).
44. Li, S., Yang, Y., Huang, S., He, Z., Li, C., Li, D., Ke, B., *et al.*, Adsorption of humic acid from aqueous solution by magnetic Zn/Al calcined layered double hydroxides. *Appl. Clay Sci.*, **188**: 105414 (2020).
45. Yang, K. & Fox, J. T., Adsorption of humic acid by acid-modified granular activated carbon and powder activated carbon. *J. Environ. Eng.*, **144(10)**: 04018104 (2018).
46. Saha, P., Chowdhury, S., Gupta, S. & Kumar, I., Insight into adsorption equilibrium, kinetics and thermodynamics of malachite green onto clayey soil of Indian origin. *Chem. Eng. J.*, **165(3)**: 874–882 (2010).
47. Shen, S., Pan, T., Liu, X., Yuan, L., Zhang, Y., Wang, J. & Guo, Z., Adsorption of Pd(II) complexes from chloride solutions obtained by leaching chlorinated spent automotive catalysts on ion exchange resin Diaion WA21J. *J. Colloid Interface Sci.*, **345(1)**: 12–18 (2010).
48. MacFarlane, R. B., Molecular weight distribution of humic and fulvic acids of sediments from a north Florida estuary. *Geochim. Cosmochim. Acta*, **42(10)**: 1579–1582 (1978).
49. Kara, H., Ayyildiz, H. F. & Topkafa, M., Use of aminoprophyl silica-immobilized humic acid for Cu(II) ions removal from aqueous solution by using a continuously monitored solid phase extraction technique in a column arrangement. *Colloids Surfaces A Physicochem. Eng. Asp.*, **312(1)**: 62–72 (2008).